Pulsed Double-Electrode GMAW-Brazing for Joining of Aluminum to Steel

This pulsed double-electrode welding process proved to be a viable alternative for low-cost joining of aluminum to steel

BY Y. SHI, G. ZHANG, Y. HUANG, L. LU, J. HUANG, AND Y. SHAO

ABSTRACT

Double-electrode gas metal arc welding (DE-GMAW) is an innovative process that can reduce the heat input to workpieces and increase the energy needed to melt a given amount of wire. To join steel to aluminum for this study, the current in the DE-GMAW was pulsed to further reduce the heat input. This resulted in pulsed DE-GMAW, which can join steel to aluminum by brazing the steel and welding the aluminum. The resultant technology may thus also be referred to as double-electrode GMAW-brazing. In this paper, this novel method was demonstrated through both theoretical analysis and experimental investigation. Dissimilar materials, aluminum and steel, were joined and major parameters affecting the metal transfer in the pulsed DE-GMAW process, including bypass arc parameters and pulsing parameters, were analyzed. The strength of the resultant aluminum-steel joint samples was examined. It was found that the average shear tensile strength was about 144.85 MPa, and the maximum one was around 186.73 MPa, which was about 88.5% of the strength of the aluminum base material. Pulsed DE-GMAW can thus be considered as an alternative method for low-cost joining of aluminum to steel.

KEYWORDS

Aluminum-Galvanized Steel • Metal Transfer • Pulsed Double-Electrode Gas Metal Arc Weld-Brazing

Introduction

Structural materials applications require consideration of many factors, including properties, costs, and manufacturing processes. As a single base material often does not provide the preferred designs, combined structures with multiple materials are often preferred over a single one to provide the needed characteristics. As the most common structural ferrous and nonferrous metals that are widely and crossly used, effective joining of steel to aluminum significantly affects the manufacturing industry. However, they possess very different physical properties, which cause difficulties in joining them together soundly.

Joining aluminum to steel has attracted significant attention from the welding research community and various application areas. Much research has been done to explore and utilize novel joining methods to achieve the joining of these dissimilar materials, such as brazing (Refs. 1, 2), laser beam welding (Refs. 3–5), electron beam welding (Ref. 6), diffusion welding (Ref. 7), and friction welding (Refs. 8, 9). Some methods were applied successfully. However, improvements are still needed in certain areas, including high cost, limited application environment, and low efficiency. Arc welding, especially gas metal arc welding (GMAW), is a highly productive joining process widely used in industrial applications (Ref. 10). Utilizing an arc welding process to achieve sound aluminum and steel joints thus becomes a critical capability for further adoption of aluminum-steel combined structures.

An important issue for effective aluminum and steel joining is the capability of lowering/controlling the heat input to the workpieces to reduce formation of detrimental intermetallic compounds at the interface. This requires that the average welding current be controlled at a small level while still maintaining the arc stability and preferred metal transfer (Ref. 11). However, typical pulsed GMAW processes have difficulty in providing such a capability. Recently, novel arc welding methods as modifications to traditional processes have been developed to provide such a capability, including methods that control welding current waveforms to reduce the arc energy such as Cold Arc by EWM (Refs. 12, 13) and QUINTO CP by CLOOS (Ref. 14). In particular, Cold Metal Transfer (CMT) is a process de-

Y. SHI (shiyu73@gmail.com), *G. ZHANG, L. LU, and J. HUANG are with State Key Laboratory of Advanced Processing and Recycling of Nonferrous Metals, Lanzhou University of Technology, Lanzhou, P. R. China. Y. HUANG is with RoMan Engineering Services, Livonia, Mich., and Y. SHAO is with University of Kentucky, Lexington, Ky.*

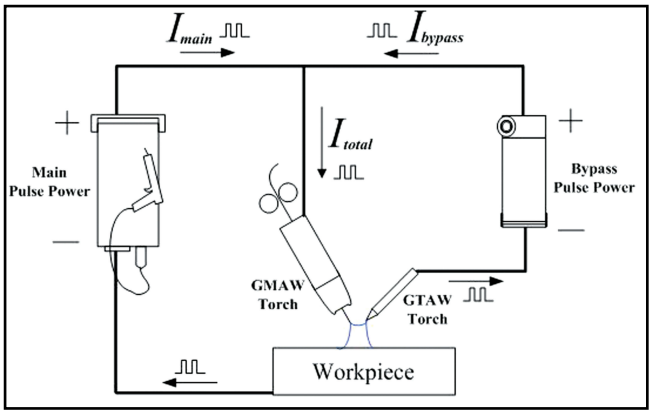

Fig. 1 — Schematic of the pulsed double-electrode GMAW process.

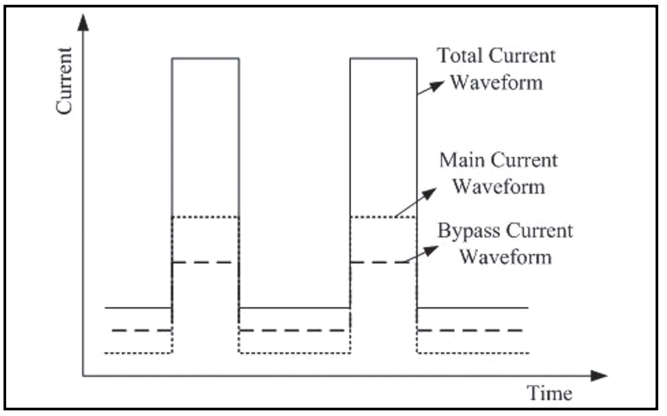

Fig. 2 — Schematic image of the designed synchronized pulsed welding current waveforms.

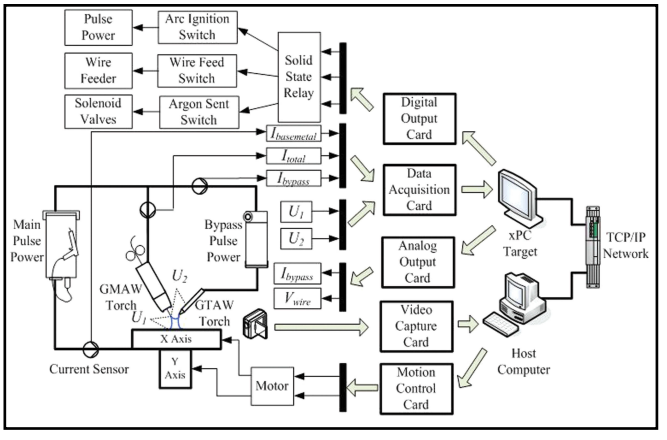

Fig. 3 — Schematic configuration of the control system in pulsed double-electrode GMAW.

veloped and patented by Fronius that utilizes a mechanical device to control the movement of the welding wire based on control of the welding current waveform. However, all these technologies bring undesirable side effects such as complicated designs, high costs, and relatively narrow welding parameter windows. Hence, exploring a novel arc welding process with lower costs and convenient control is still essential for the joining of dissimilar aluminum and steel.

Double-electrode GMAW is a newly developed, highly efficient, novel arc welding process (Refs. 15–20). In this process, a bypass gas tungsten arc welding (GTAW) torch is added to the traditional GMAW system to bypass part of the current through the base material. In this way, the heat input to the base material is reduced, and by adjusting and controlling the bypass current, the heat input to the workpiece can be well controlled. The desirable stable metal transfer can be obtained even when the heat input is low. In addition, the bypass arc not only benefits increasing the efficiency of welding but also control of the welding thermal process and metal transfer (Refs. 21–25). Compared to the CMT process, the complicated mechanical equipment to pull and push the welding wire to assist the metal transfer is no longer needed. From the schematic configuration given in Ref. 26, two power supplies and two welding guns are used. While the complexity is slightly increased, the requirement on the dynamic characteristics of the power supply is not high and the cost of the system is reduced. Furthermore, a specialized all-in-one power supply can be made and a controllable rectified switch bridge can replace the bypass loop power supply; the two welding guns can also be integrated together to be compact.

Table 1 — Average Main and Bypass Loop Currents Used in Experiments

Bypass loop average current \ Main loop average current	24 A	30 A	35 A	40 A	45 A	50 A	55 A	60 A
28 A	√	√	√	√	√	√	√	√
32 A	√	√	√	√	√	√	√	√
37 A	√	√	√	√	√	√	—	—
40 A	√	√	√	√	√	√	—	—
45 A	√	√	√	√	√	—	—	—
50 A	√	√	√	√	—	—	—	—
55 A	√	√	√	√	—	—	—	—
60 A	√	√	√	√	—	—	—	—

Note: '√' = satisfactory formation of Al-steel weld obtained, and '—' = no experiment.

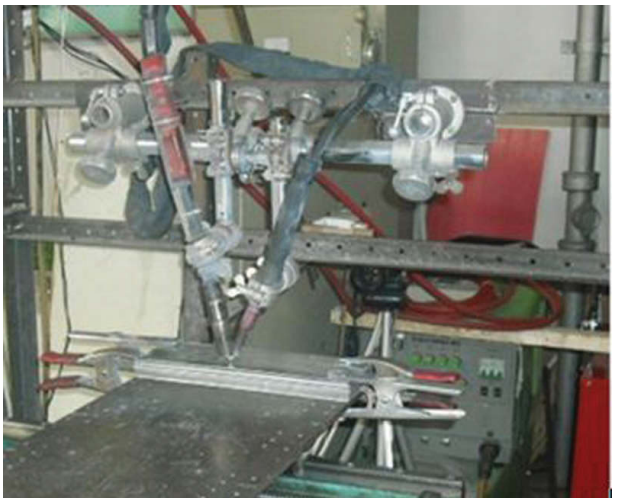

Fig. 4— Experimental setup.

Fig. 5 — Aluminum-steel bead-on-plate weld beads made with double-electrode GMAW (I_{bypass} = 30 A, I_{main} = 32 A, I_{mp} = 167 A, I_{mb} = 10 A, I_{bp} = 104 A, I_{bb} = 18 A, T_p = 1.75 ms, T_b = 10.75 ms, V_{wire} = 4.47 m/min). A — Without current pulsing; B — with current pulsing.

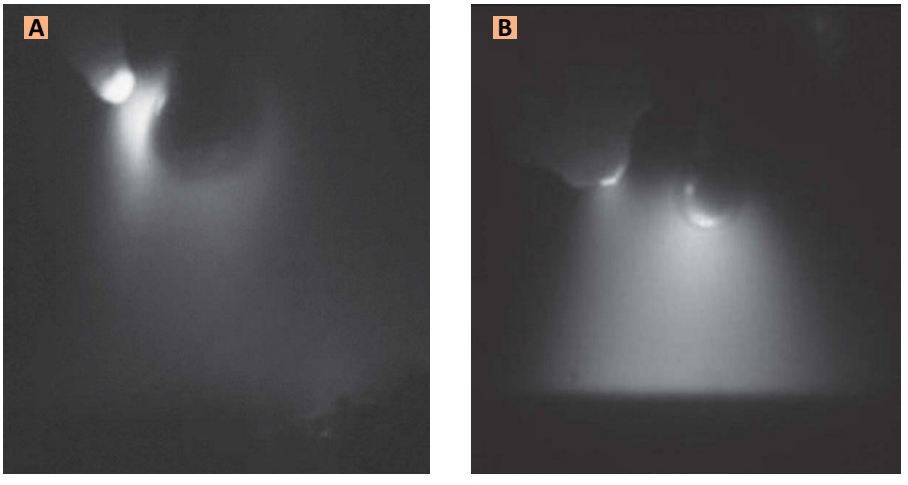

Fig. 6 — Typical metal transfer in double-electrode GMAW for joining dissimilar aluminum-steel. A — Without current pulsing; B — with current pulsing.

This novel process can thus be applied with reasonable equipment size, cost, and structure. Unfortunately, introducing the bypass gun alone does not satisfy the requirements for the joining of dissimilar aluminum and steel.

For low heat input applications, the applicable window for bypass welding parameters is still relatively narrow and the heat input needs to be further reduced.

Based on the previous theoretical and application studies, to better meet the requirements of dissimilar aluminum and steel joining (low heat input and stable metal transfer process) (Refs. 27, 28), a pulsed current waveform was introduced in this paper to the novel DE-GMAW system. For the novel pulsed double electrode GMAW-brazing proposed in this paper, the main and bypass arc currents were both pulsed. A digital control system was developed to control the wire feed speed, synchronization of the main and bypass current waveforms, and other system parameters. The required detaching forces for metal transfer and heat input to workpiece to generate the needed weld pool on the similar base metals can thus be effectively controlled.

Experimental Setup

Figure 1 schematically illustrates the principle of the pulsed DE-GMAW system. Analysis shows that the currents satisfy the following relations:

Table 2 — Effects of Peak and Base Currents on Metal Transfer

Main Loop Bypass Loop	I_{mp} = 198 A, I_{mb} = 5 A	I_{mp} =167 A, I_{mb} = 10 A	I_{mp} = 136 A, I_{mb} = 15 A	I_{mp} = 106 A, I_{mb} = 20 A	I_{mp} = 75 A, I_{mb} = 25 A	I_{mp} = 32 A, I_{mb} = 32 A
I_{bp} = 104 A, I_{bb} = 18 A	MTF:80Hz	MTF: 80 Hz	MTF: 72 Hz	MTF: 24 Hz	MTF: 19 Hz	Globular and short-arc transfer, unstable process
I_{bp} = 67 A, I_{bb} = 24 A	MTF: 80 Hz	MTF: 62 Hz	MTF: 17 Hz	MTF: 10 Hz	MTF: 1 Hz	Unstable welding process
I_{bp} = 30 A, I_{bb} = 30 A	MTF: 65 Hz	MTF: 10 Hz	MTF: 1 Hz	Unstable process	Unstable process	Unstable welding process

* MTF: free-flight Metal Transfer Frequency average; I_{bypass} = 30 A, I_{main} = 32 A, $V_{welding}$ = 0.5 m/min, duty ratio δ = 14%, pulse frequency f = 80 Hz. Results with MTF less than 80 Hz, synchronized with the waveform frequency of the currents indicate successful free flight transfer.

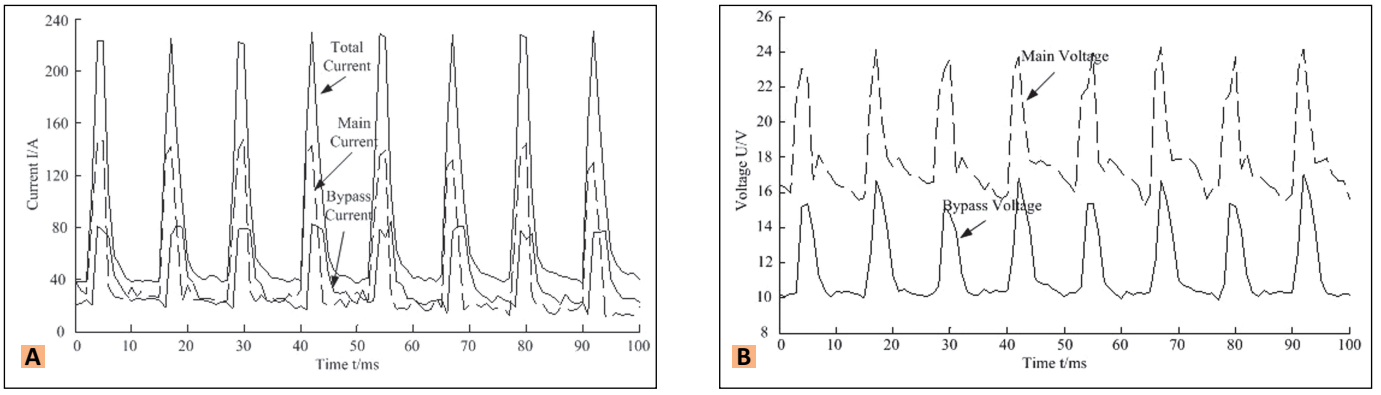

Fig. 7 — Typical current and voltage waveforms (I_{bypass} = 32 A, I'_p = 85 A, I'_b = 18.5 A; I_{main} = 45 A, I_p = 145 A, I_b = 20A; δ = 20; f = 80 Hz; V_{wire} = 5.7 m/min). A — Current; B — voltage.

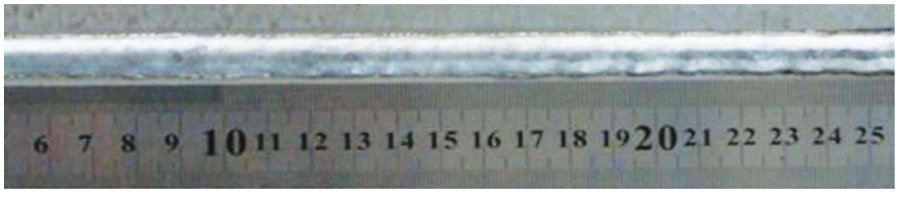

Fig. 8 — Weld surface in bead-on-plate dissimilar aluminum-steel joining.

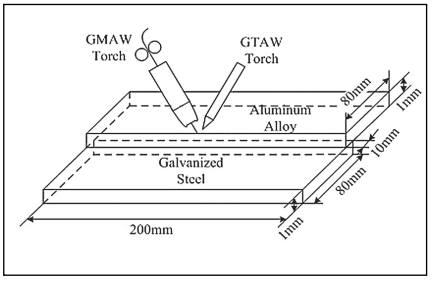

Fig. 9 — Aluminum-steel lap-joint design for pulsed double-electrode GMAW-brazing.

Equation 1 ~ 5. DE-GMAW has been proven to be able to produce the desired spray transfer at low base metal currents (Ref. 28). By introducing pulsed welding current waveforms (shown in Fig. 2), the ability to achieve the desired metal transfer can be further enhanced without changing the average currents in the main and bypass loops to satisfy the requirements to detach droplets at the low base material heat inputs that are needed to join dissimilar aluminum and steel. It can also reduce the requirements on the dynamic characteristics of the power supply and on the specific signal processing. The desired spray metal transfer could be achieved when the average current is far below the transition current (Refs. 29, 30) in the traditional GMAW process. To easily realize and set up pulsed double-electrode GMAW-brazing for the aluminum to steel joining experiments, an experimental system was established using the fast control model technology, as shown in Fig. 3.

In the experimental system, the main power supply is a DALEX VIRO MIG-400L pulsing digital machine manufactured in Germany, and the bypass power supply is a digital pulsing machine with open connectors. Other elements include an X-Y double-axle welding table, and MC6212 motion control board. The visual acquisition system includes a Panasonic CP-230 CCD camera, an NI PCI-1405 image acquisition board, a GZL-CL-22C5M-C high-speed CCD camera, and a high-speed image acquisition board from Point Grey Research Co. Optical devices include a zoom lens and a lens with a neutral dimmer filter, a narrow-band filter, and heat reduction filter. The data acquisition for electrical signals and the output system consist of a real-time target system made of two industrial control computers, a PCL-812PG data acquisition board that supported xPC environment, a PCL-728 D/A output board with isolation, a CSM400FA closed-loop current sensor, and ADAM-3014 standard voltage isolation modules.

The host computer was connected to the target xPC by TCP/IP protocol. The host computer was used for the

Table 3 — Effects of Pulse Duty Ratio and Base Currents on Metal Transfer

Duty Ratio	18%		16%		14%		12%		10%		8%	
Base Current	Main 9 A	Bypass 17 A	Main 12 A	Bypass 18.4 A	Main 15 A	Bypass 20 A	Main 18 A	Bypass 22 A	Main 20 A	Bypass 23 A	Main 23 A	Bypass 25 A
Metal Transfer Frequency	80 Hz		80 Hz		58 Hz		34 Hz		Occasional short-arc transfer, 12 Hz		Occasional short-arc transfer, 5 Hz	

*I_{bypass} = 30 A, I_{main} = 32 A, $V_{welding}$ = 0.5 m/min, pulse frequency f = 80 Hz, I_{mp} = 136 A, I_{bp} = 91 A. Results with MTF less than 80 Hz, synchronized with the waveform frequency of the currents indicate successful free flight transfer.

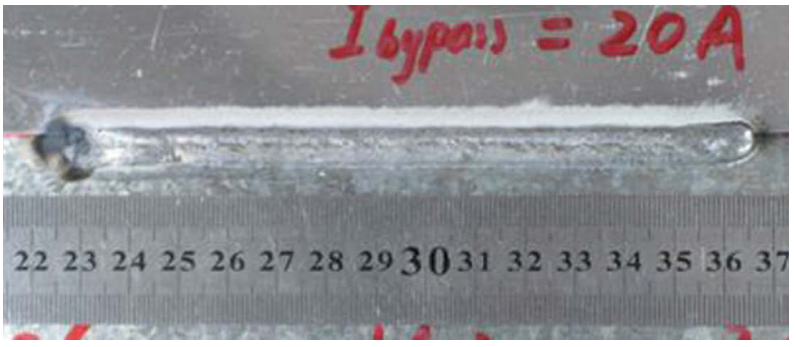

Fig. 10 — Aluminum-steel lap-joint surface image in pulsed double-electrode GMAW-brazing (I_{total} = 50 A, I_{main} = 30 A, I_{bypass} = 20 A, V_{wire} = 3.05 m/min, $V_{welding}$ = 0.5 m/min).

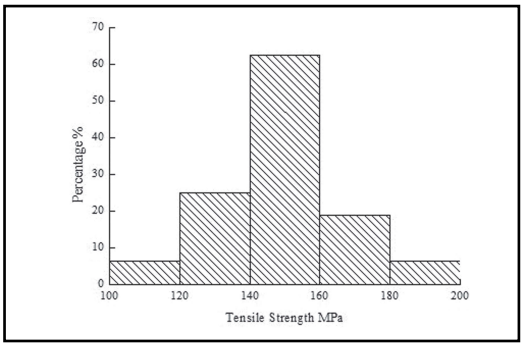

Fig. 11 — Strength distribution of aluminum-steel lap-joint samples.

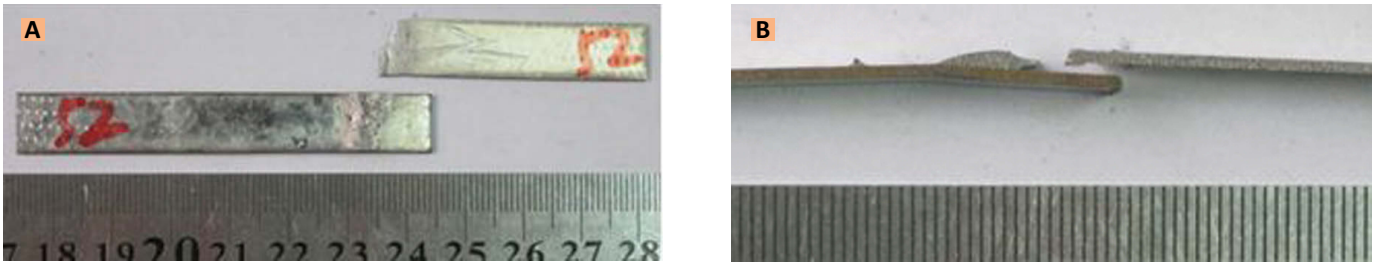

Fig. 12 — Ruptured position in 5052 aluminum and galvanized steel lap joint (tensile strength was 186.73 MPa) (I_{total} = 54 A, I_{main} = 38 A, I_{bypass} = 16 A, $V_{welding}$ = 0.6 m/min). A — Front view; B — side view.

control algorithm compiling and debugging, acquisition of visual images, motion control of the XY double-axle work table, and data analysis processing and storage. The target machine was used to execute the setting algorithm, which included signal acquisition and real-time display of the welding current and voltage, the signals for arc ignition, motion of wire feeder, and shielding gas feeding, and output of control signals, etc. The cooperation based on division of labor of host and target computer machines made the experimental system possess high real-time ability and fast response speed.

The system can realize control and adjustment of the main and bypass loop welding current waveforms, and collect the welding electric signals and visual signals in the aluminum-steel joining process. The visual signals can be collected, displayed, processed, and stored. By processing and analyzing the collected welding signals and using the control algorithm, the output signals can be controlled in real time. The welding parameters for aluminum-steel welding can be optimized, and thus the joining process of these dissimilar materials can be appropriately controlled. Figure 4 shows the experimental system.

Figure 5 shows the bead-on-plate dissimilar aluminum-steel welds, made by melting and depositing aluminum wire on steel, with and without pulsing the welding current waveforms for low average currents (32 and 30 A for the main and bypass loops, respectively). The filler material used was ER5356 aluminum filler metal and the steel base metal was galvanized steel with zinc thickness at 100 g/m^2. The travel speed $V_{welding}$ was 0.5 m/min. Figure 6 shows the corresponding metal transfer images obtained by the high-speed camera. From Figs. 5A and 6A where the currents were not pulsed, it can be seen that when the average currents are low, it is difficult to form aluminum-steel bead-on-plate welds. The droplet size was too large and the desirable free-

Table 4 — Effects of Pulse Duty Ratio and Peak Currents on Metal Transfer

Duty Ratio	30%		26%		22%		18%		10%		6%	
Peak Current	Main 83 A	Bypass 58 A	Main 95 A	Bypass 64 A	Main 110 A	Bypass 73 A	Main 132 A	Bypass 85 A	Main 230 A	Bypass 138 A	Main 377 A	Bypass 218 A
Metal Transfer Frequency	Occasional Short-arc transfer, 2 Hz		Occasional Short-arc transfer, 10 Hz		27 Hz		52 Hz		80 Hz		Limited by the power supply	

* I_{bypass} = 30 A, I_{main} =32 A, $V_{welding}$ = 0.5 m /min, pulse frequency f = 80 Hz, I_{mb} = 10 A, I_{bb} = 18 A. Results with MTF less than 80 Hz, synchronized with the waveform frequency of the currents indicate successful free flight transfer.

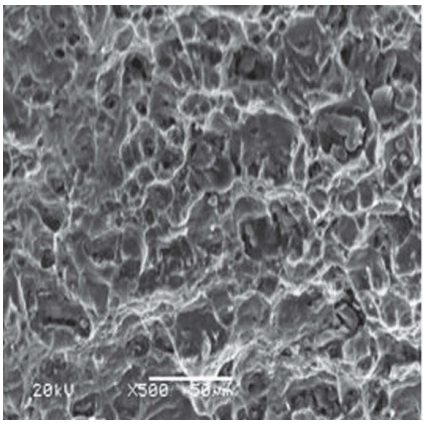

Fig. 13 — Surface morphology of ruptured 5052 aluminum and galvanized steel lap joint.

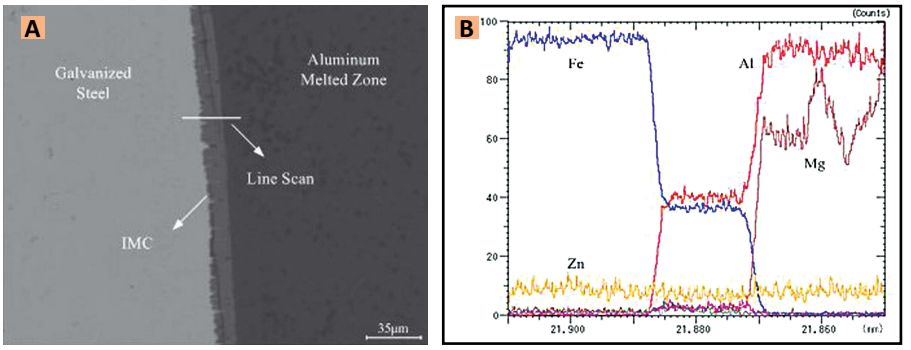

Fig. 14 — Linear scanning of the joint interface. A — Scanning position; B — element distribution at the interface.

flight metal transfer was difficult to achieve. After the currents were pulsed, the desirable, stable free-flight metal transfer was achieved as shown in Figs. 5B and 6B. The diameter of the droplet was almost the same as the one of the filler metals resulting in smooth formation of welds on the steel and aluminum. The effectiveness in using the pulsed currents to improve metal transfer in the DE-GMAW process is thus experimentally verified together with the developed experimental system.

Pulsed DE-GMAW Process and Analysis

The bead-on-plate weld was adopted in the analysis for the pulsed DE-GMAW process. The base material was the galvanized steel (Q235 low-carbon steel base) with Zn thickness at 100 g/m^2, and the coupon size was 300 × 100 × 2 mm. The filler metal was 1.2-mm-diameter ER5356 aluminum. Pure argon was used for shielding gas and the flow rates for the main and bypass loop were 20 and 5 L/min, respectively. The coupons were cleaned with acetone before welding to remove oil and stains on the surface. The position of and angle between the main and bypass guns were appropriately adjusted to make sure that stably coupled main and bypass arcs were maintained.

To preliminarily determine the welding parameter window in pulsed DE-GMAW for aluminum-steel dissimilar joining, the following experiments were designed: Eight values for the average main and bypass currents respectively were selected, and then cross-matching experiments were conducted. The travel speed was kept at 0.5 m/min. The wire feed speed was on-line adjusted based on the change in the currents. The frequency of the pulses was constant and was set at 80 Hz. Table 1 shows the average main and bypass welding currents adopted in these experiments. From Table 1, it was found that there was a wide parameter window for aluminum-steel bead-on-plate welding in the pulsed DE-GMAW process. With the welding process controlled, satisfactory aluminum-steel bead-on-plate welds could be effectively achieved even when the average base and bypass currents were 24 and 28 A, respectively.

Figure 7 shows a group of typical current and voltage waveforms sampled each 100 ms. From Fig. 7A, the current pulses for the main and bypass loop were almost synchronized. Because of the response time between the welding power supply and control loop, there was a delay in the bypass current pulse, which is approximately 1–2 ms, whose effect on the aluminum-steel welding process may be negligible. As the impulses of the main and bypass loop currents were exerted at the same time, it was the peak current that would further reduce the transition current for spray metal transfer of aluminum. Figure 7B is the corresponding voltage waveform. The main loop voltage was measured between the GMAW gun (contact tip) and the workpiece, and the bypass one was between the main GMAW gun and the bypass tungsten. Figure 8 shows the corresponding surface of the resultant aluminum-steel bead-on-plate welds. It can be seen that with this set of parameters, uniform weld width and smooth weld surface were produced.

The main advantage of the pulsed DE-GMAW process is that it can realize stable free-flight metal transfer with quite low heat input to the base materials. There are two major reasons: 1) Because of the bypass loop arc, beside the effect of reducing the heat input to the base materials, the bypass arc also changes the distribution of the electromagnetic force to enhance the metal transfer and reduce the transition current needed for the droplet to freely transfer; 2) because of the bypass current, by utilizing the synchronized and controlled main and bypass current waveforms, the average main and bypass currents can be kept almost the same, even smaller, while still effecting the desired metal transfer. As such, the average main and bypass currents could be further reduced, and the heat input to the base materials could also be further reduced.

The references (Ref. 28) analyzed the forces exerted on the droplet in the double bypass electrode GMAW process. First, the radial direction of the electromagnetic force due to the bypass arc could accelerate the pinch effect of the droplet, and the axial direction of this force can enhance droplet detachment. Second, because of the bypass arc, the root of the main arc could easily extend to wrap the droplet, thus further making the electromagnetic force on the droplet to detach the molten metal and strengthening the detaching force. Last, the plasma drag force from the bypass arc will generate an additional detaching force and accelerate droplet detachment, and then the plasma drag

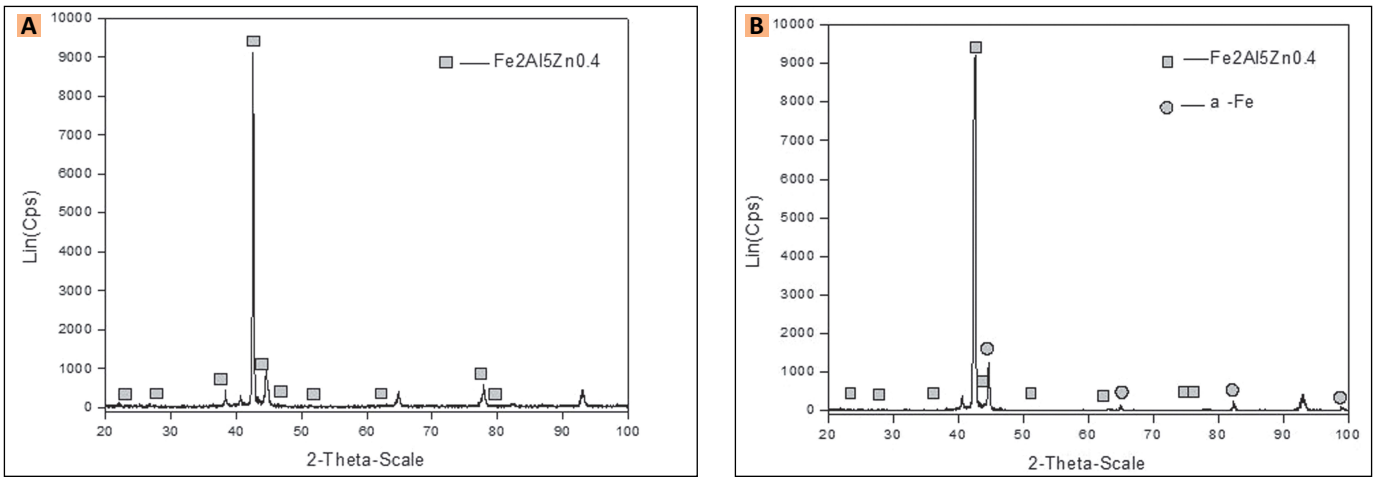

Fig. 15 — XRD analysis of the ruptured surface of aluminum and galvanized steel side samples. A — Ruptured surface on the aluminum side; B — ruptured surface on the galvanized steel side.

force would be increased, which will benefit the droplet detachment from the wire. In addition, by adjusting and controlling the bypass current, the arc force on the droplet and arc shape could be changed, and thus different metal transfer processes could be achieved. The transition current for spray metal transfer could be reduced, and thus free-flight metal transfer could be obtained with low heat input to the base materials.

To further reduce the heat input to base materials and keep the stable metal transfer, the pulsing current was introduced to this novel method. By synchronizing the main and bypass loop current pulses and controlling the process parameters, the droplet would be detached at the peak current in both the main and bypass loops, and the arc would be maintained when the current was at the base ones to maintain the arc, preheat base material and filler metal, and not generate droplet transfer. It was essential to keep the stable metal transfer in order to use DE-GMAW to effectively GMAW-braze aluminum-steel.

The effects of the pulse current parameters, under the same average main and bypass currents, on the free-flight droplet transfer was studied using high-speed images. The results are summarized in Tables 2–4 where results with an observed transfer frequency synchronized with that of the current waveform imply successful free-flight transfer was produced. As can be seen, increases in the peak currents (main and bypass currents) as well as in the durations, all benefit the free-flight metal transfer. Further, the peak currents have more significant effects on droplet detachment than pulse duty ratio. For relatively small average currents, the pulse parameters can be adjusted by such as increasing the peak current level and/or peak time in the main and bypass loops, to obtain free-flight metal transfer. The main effect of the base current is to main the arcs and preheat the base material and filler metal. The main and bypass loop base currents thus could be set at low levels to reduce the heat input to effectively detach droplets at low heat inputs.

As can be seen, pulsed DE-GMAW provides an effective method for producing the desired free-flight transfer at extremely low currents and heat input, and melt aluminum wire to deposit on steel. It promises an effective method for joining aluminum to steel. As will be seen in the next section, this process can join similar metals (aluminum and steel) by welding aluminum and brazing steel to result in double-electrode GMAW-brazing of aluminum-steel.

Double-Electrode GMAW-Brazing of Aluminum-Steel

Lap-Joint Experiments

The base metal materials were the galvanized steel (Q235 low-carbon steel) with zinc thickness of 100 g/m^2 and 5052 aluminum alloy. The coupon size was 200 × 80 × 1 mm for both materials. The aluminum was lapped on the top of the galvanized steel, and the lap width was 10 mm. The filler metal was 1.2-mm-diameter 4043 (AlSi5) aluminum. Pure argon was used as the shielding gas, and the flow rates for the main and bypass loops were 20 and 5 L/min, respectively. The coupons were cleaned with acetone before welding to remove oil and stains on the surface. Then the two coupons were clamped to the welding table. It was also necessary to make sure the main and bypass guns were at the same plate. The angle between the two guns also had to be appropriately adjusted, and the tip of the welding wire pointed to the right position. The schematic configuration of the lap joint and lap width are shown in Fig. 9.

Figure 10 shows the typical formation of an aluminum-steel lap joint made using the pulsed DE-GMAW process. It was found that a satisfactorily smooth-surfaced lap joint could be obtained. The amount of the zinc burnt was quite small, and the distortion was also insignificant. The total (average) welding current through the filler metal was approximately 50 A, and the average main and bypass loop currents were approximately 30 and 20 A, respectively. This indicates that by optimizing the bypass arc and pulse current parameters, stable metal transfer and satisfactory formation of an aluminum-steel joint could be achieved at low currents in pulsed double-electrode GMAW for GMAW-brazing of aluminum-steel.

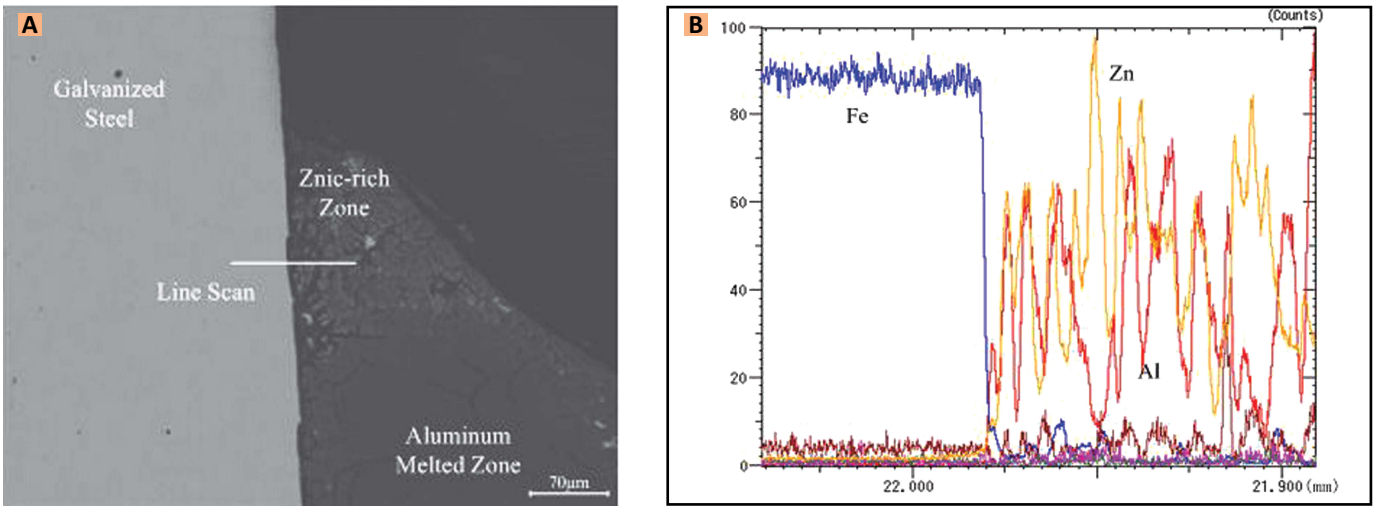

Fig. 16 — Linear scanning of the Zn-rich zone. A — Scanning position; B — element distribution in the Zn-rich zone.

Strengths

Strength tests were conducted on the 5052 aluminum and galvanized steel lap-joints. Figure 11 shows the shear tensile strength distribution for the 20 lap-joint samples. From Fig. 11, the lap joint shear tensile strength is in the range from 120 to 180 MPa, and the average and maximum strengths are 144.85 and 186.73 MPa, respectively. It is approximately 88.5% of that of the aluminum base material (the tensile strength of 5052 aluminum is about 211 MPa). This indicates that the intrinsic strength of the aluminum-steel lap joint was larger than 144.85 MPa in pulsed double-electrode GMAW-brazing.

During the shear tensile tests, the samples were mainly ruptured at the heat-affected zone (HAZ) on the aluminum side. This is mainly because the crystal grains in the HAZ are prone to grow to a large size during the welding process, and further become soft and reduce the mechanical properties, as shown in Fig. 12. Figure 13 shows the corresponding surface morphology of shear tensile ruptured samples. It was found that the rupture mode is a ductile one.

Microstructure Analysis

Figure 14A shows the SEM interface images of the aluminum-steel joint. From Fig. 14A, it can be found that a layer of intermetallic compounds about 10 um thick was formed between the aluminum fusion zone and base galvanized steel. These kinds of intermetallic compounds formed their grain cores at the interface, and grew into the base steel in the shape of columnar grains. To further analyze the composition of the intermetallic compound at the interface, linear scanning of the joint was conducted as shown in Fig. 14B. From Fig. 14B, it can be seen that these compounds mainly consisted of Al and Fe elements. From the galvanized steel base metal to the central interface in the scanning zone, the content of Fe decreased dramatically, but the content of Al increased rapidly. Along the central interface, the Fe and Al contents were both relatively constant, and there was an obvious plain stage. The zinc was uniformly distributed in the entire joint.

To further determine the intermetallic compound at the interface, the joint was sheared apart. An X-ray diffraction test was conducted on the ruptured surfaces of the aluminum and steel samples, and the results are shown in Fig. 15. From Fig. 15, it could be found that the intermetallic compounds consisted of $Fe_2Al_5Zn_{0.4}$ and Fe. Combined with the aforementioned linear analysis results, the uniform and continuous phase at the interface was $Fe_2Al_5Zn_{0.4}$. According to other studies (Refs. 31–33), the $Fe_2Al_5Zn_{0.4}$ is supposed to form when the intermetallic compound Fe_2Al_5 interacts with the dissolved Zn at the interface.

As the melting and boiling points of Zn are very low (419.5 and 907, respectively) (Ref. 34), with the heat effect from the electric arc, the Zn coating is prone to evaporate. In this case, the content of Zn at the center area was very low due to the high arc temperature. At the surrounding area of the electric arc, a portion of unevaporated Zn was accumulated at the boundary of the weld joint at the effect of electric arc force. They interacted with the molten aluminum droplet and formed a Zn-rich zone at the toe of the weld, as shown in Fig. 16A. Figure 16B shows the linear scanning of the Zn-rich zone for element distribution, which also demonstrates that the Zn indeed accumulated at this zone and Zn-Fe solid solution was formed.

Conclusions

1. The novel DE-GMAW process, which provides a convenient way to effectively control heat input and metal transfer, was modified by pulsing the currents to form the novel pulsed DE-GMAW process. The pulsed DE-GMAW process further reduces heat input and enables double-electrode GMAW-brazing of aluminum-steel.

2. An experimental system was established to implement the novel pulsed DE-GMAW process. It controls and synchronizes the main and bypass loop current waveforms to provide the needed parameters to GMAW-braze aluminum-steel.

3. Effective ways to realize stable free-flight metal transfer at the low current include increasing the bypass loop

current as well as increasing the peak current and duration both in the main and bypass loops. The base currents in both the main and bypass loops can be set at relatively low levels to further reduce heat input.

4. The average and maximum strengths for the aluminum-steel lap joints are 144.85 and 186.73 MPa, respectively.

5. The intermetallic compounds at the interface of the aluminum-steel lap joint mainly consist of uniformly distributed Fe_2Al_5 or Fe_2Al_5ZnX at the steel side, and the $FeAl_3$ in needle flake at the aluminum side. At the toe of the joint, there is a Zn-rich zone and the main content was Al-Fe solid solution.

Acknowledgments

This work was funded by the National Natural Science Foundation of China (#51165023), financial commission of Gansu Province of China and the Key Project of Chinese Ministry of Education (#210229); Projects of International Cooperation and Exchanges NSFC (#51210105024); Financial Commission of Gansu Province of China, and the Hong Liu Outstanding Talent Training Plan of Lanzhou University of Technology of China (#J201201).

References

1. Saida, K., Song, W., and Nishimoto, K. 2005. Diode laser brazing of aluminium alloy to steels with aluminium filler metal. *Science and Technology of Welding & Joining* 10(2): 227–235.

2. Gang, D. H., Liao, C., Chen, G. et al. 2012. Butt joining of aluminum to steel by arc brazing process. *Materials and Manufacturing Processes* 27(12): 1392–1396.

3. Mathieu, A., Shabadi, R., Deschamps, A., et al. 2007. Dissimilar material joining using laser (aluminum to steel using zinc-based filler wire). *Optics & Laser Technology* 39: 652–61.

4. Ozakia, H., Kutsuna, M., Nakagawa, N., et al. 2010. Laser roll welding of dissimilar metal joint of zinc coated steel to aluminum alloy. *Journal of Laser Applications* 22(1): 1–6.

5. Rathod, M. J., and Kutsana, M. 2004. Joining of aluminum alloy 5052 and low carbon steel by laser roll welding. *Welding Journal* 83(1): 16-s to 26-s.

6. Franc, A. 2007. Low energy welding of heterogeneous joints between steel and aluminum. Soutěžní prehlídka studentských a doktorských prací fst.

7. Goecke, S. F. 2005. Low energy arc joining process for materials sensitive to heat. EWM *Hightec Welding* 11: 1–5.

8. Uzun, H., Donne, C., and Argagnotto, A. 2005. Friction stir welding of dissimilar Al6013-T4 to X5CrNi18-10 stainless steel. *Materials and Design* 26(1): 41–46.

9. Kimapong, K., and Watanabe, T. 2005. Lap joint of A5083 aluminum alloy and SS400 steel by friction stir welding. *Materials Transactions* 46(4): 835–841.

10. Tetsu, I., Seiji, S., Tsuyoshi, M., et al. 2008. Dissimilar metal joining of aluminum alloys and steel in the spot welding by using advanced hot-dip aluminized steel sheet. *Kobelco Technology Review* 28: 29–34.

11. Shi, Y., Shao, L., Huang, J., et al. 2013. Effects of Si and Mg elements on the microstructure of aluminum-steel joints produced by pulsed DE-GMA welding-brazing. *Materials Science and Technology* 29(9): 1118–1124.

12. Bruekner, J. 2005. Cold metal transfer has a future joining steel to aluminum. *Welding Journal* 84(6): 38–40.

13. Furukawa, K. 2006. New CMT arc welding process — welding of steel to aluminum dissimilar metals and welding of super-thin aluminium sheets. *Welding International* 20(6): 440–445.

14. Kochan, A. 2006. Welding innovations for thick and thin sheet. *Assembly Automation* 26(4): 273–274.

15. Li, K. H., Chen, J. S., and Zhang, Y. M. 2007. Double-electrode GMAW process and control. *Welding Journal* 86(8): 231–237.

16. Wei, H. L., Li, H., Yang, L. J., et al. 2013. Consumable double electrode with a single arc GMAW. *International Journal of Advanced Manufacturing Technology* 68(5): 1539–1550.

17. Wu, C. S., Hu, Z. H., and Zhong, L. M. 2012. Prevention of humping bead associated with high welding speed by double-electrode gas metal arc welding. *International Journal of Advanced Manufacturing Technology* 63(5): 573–581.

18. Ma, G., and Zhang, Y. M. 2012. A novel DE-GMAW method to weld steel tubes on simplified condition. I*nternational Journal of Advanced Manufacturing Technology* 63(5): 147–153.

19. Shi, Y., Han, R.-H., Huang, J.-K., et al. 2012. Numerical simulation of temperature field of DE-GMAW and its comparison with experimental measurements. *Acta Physica Sinica* 61(2): 020205.

20. Li, K., and Zhang, Y. M. 2010. Interval model control of consumable double-electrode gas metal arc welding process. *IEEE Transaction on Automation Science and Engineering* 7(4): 826–839.

21. Li, K., and Wu, C. 2009. Mechanism of metal transfer in DE-GMAW. *Journal of Materials Science and Technology* 25(3): 415–418.

22. Li, K. H., Zhang, Y. M., Xu, P., et al. 2008. High-strength steel welding with consumable double-electrode gas metal arc welding. *Welding Journal* 87(3): 57-s to 64-s.

23. Li, K. H., and Zhang, Y. M. 2008. Consumable double-electrode GMAW Part II: Monitoring, modeling, and control. *Welding Journal* 87(2): 44-s to 50-s.

24. Li, K. H., and Zhang, Y. M. 2008. Consumable double-electrode GMAW — Part 1: The process. *Welding Journal* 87(1): 11-s to 17-s.

25. Zhou, W. Z., and Zhang, Y. M. 2007. Image processing algorithm for automated monitoring of metal transfer in double-electrode GMAW. *Measurement Science and Technology* 18(7): 2048–2058.

26. Zhang, Y. M., Jiang, M., and Lu, W. 2004. Double electrodes improve GMAW heat input control. *Welding Journal* 83(11): 39–41.

27. Shi, Y., Liu, X. P., and Zhang, Y. M. 2007. Dual-bypass GMAW of aluminum — Minimizing base metal heat input with good welding quality. *Proceedings FABTECH International & AWS Welding Show*, pp. 223–226.

28. Shi, Y., Liu, X. P., Zhang, Y. M., and Johnson, M. 2008. Analysis of metal transfer in dual-bypass GMAW of aluminum. *Welding Journal* 87(9): 229–236.

29. Li, K., and Zhang, Y. M. 2007. Metal transfer in double-electrode gas metal arc welding. *Journal of Materials Science and Technology — Transactions of the ASME* 129(6): 991–999.

30. Shi, Y., Chen, Z., Xue, C., et al. 2010. Research on metal transfer in dual bypass MIG welding of aluminum [J]. *Journal of Mechanical Engineering* 46(20): 76–79.

31. Shi, Y., Wang, Z., Huang, J., et al. 2013. Study on microstructure of fusing-brazing joint of aluminum to galvanized steel by pulsed ED-GMAW [J]. *Transactions of the China Welding Institution* 34(5): 1–4.

32. Zhang, H. T., Feng, J. C., He, P., et al. 2007. Interalfacial microstructure and mechanical properties of alumimum-zinc-coated steel joints made by a modified metal inert gas welding-brazing process [J]. *Material Characteristics* 58: 588–592.

33. Song, J. L., Lin, S. B., Yang, C. L., et al. 2009. Spreading behavior and microstructure characteristics of dissimilar metals TIG welding-brazing of aluminum alloy to stainless steel [J]. *Material Science and Engineering* A 509: 31–40.

34. Wu, C. S. 2007. Welding thermal processes and weld pool behaviors [M]. *Beijing, China Machine Press*.

Appendix

$$I_{total} = I_{main} + I_{bypass} \quad (1)$$

$$I_{tp} = I_{mp} + I_{bp} \quad (2)$$

$$I_{tb} = I_{mb} + I_{bb} \quad (3)$$

$$T_{tb} = T_{mp} - T_{bp} \quad (4)$$

$$T_{tb} = T_{mb} - T_{bb} \quad (5)$$

where I_{total} is the total current through the welding wire, I_{main} is the average main current, I_{bypass} is the average bypass current, I_{tp} is the peak current through the welding wire, I_{mp} is the main loop peak current, I_{bp} is the bypass loop peak current, I_{tp} is the base current through the welding wire, I_{mb} is the main loop base current, I_{bb} is the bypass loop base current, T_{tp} is the time of the peak pulse current through the welding wire, T_{mp} is the main loop peak current time, T_{bp} is the bypass loop peak current time, and T_{tb} is the time of the base pulse current through the welding wire, T_{mb} is the main loop base current pulse time, and T_{bb} is the bypass loop base current pulse time.